Relative-Air Humidity Sensing Element Based on Heat Transfer of a Single Micromachined Floating Polysilicon Resistor

P. Zambrozi Jr. and F. Fruett

School of Electrical and Computer Engineering – FEEC, University of Campinas, Campinas, São Paulo, Brazil
e-mail: paulo.zambrozi@lnnano.org.br and fabiano@dsif.fee.unicamp.br

ABSTRACT

An air-humidity sensing element based on heat transfer mechanisms (conduction and convection) is presented. The sensing element is a single floating resistor of doped polysilicon, which operates in two phases: thermal actuation and thermal sensing. As thermal actuation, a convenient biasing current is applied to the resistor leading its self-heating by Joule Effect. As thermal sensing, the resistor biasing current is reduced and its Thermal Time Constant (τ) during the cool-down process is measured. Characterization results show that τ is closely related to the air relative humidity (%RH). This sensor presents a maximum power consumption of 5 mW.

Index Terms: Heat transfer mechanisms, air-humidity sensor, thermal conduction, thermal convection.

1. INTRODUCTION

Heat transfer mechanisms are a dominant characteristic of nearly every energy conversion and production device being fundamental to all branches of engineering. Due to technological advances in recent decades, the mechanism of heat transfer has allowed a precise temperature control of integrated systems (from integrated circuits to data centers).

In recent decades the control and monitoring of relative humidity in industrial environments is growing due to greater availability of the circuits, the microprocessors and humidity sensors. Generally, the requirements that a humidity sensor has to meet to reach a wide range of applications are [1]: (a) sensitivity for a wide range of humidity and temperature; (b) short response time; (c) reproducibility and low hysteresis; (d) durability; (e) resistant to contaminants; (f) low temperature dependence and finally (g) low-cost. Anyway, none of the currently developed humidity sensor is able to attempt all characteristic satisfactorily.

Nowadays, it can be found in the literature several types of relative humidity sensors, varying the type of hygroscopic material used (sensitive element) until the kind of signal it works with (electric, optical, mechanical or radiant). Most humidity sensors currently used are based on resistors and capacitors [2].

The advance made in CMOS (Complementary Metal Oxide Semiconductor) has allowed to reaching others types of humidity sensors. Basically, three types of humidity sensor are found in the literature:

- Optical Humidity Sensor – these sensors are based on the variation of an electromagnetic wave (amplitude, polarization, frequency or phase) as a function of relative humidity. They are divided into two different measurements methods. The first method is the absorption which relates the characteristic of moisture absorption in the wavelength – spectrometry. The water vapour can change both amplitude and polarization of the wavelength in the range 1 to 10 μm (infrared). An example of this sensor was presented by Schirmer *et al* [3]. Besides the infrared spectrum, we also find sensors operating in the ultraviolet range – called Lyman-Alpha sensors [4]. The second method is the adsorption which relates the formation of nuclei of water on a mirror surface – called dew point. A recent development in this area occurs through the acoustic wave sensors – SAW [5].
- Capacitive Humidity Sensor – theses sensors are based on the variation of the dielectric constant of the capacitor as a function of amount of water vapour absorbed. Interdigitated electrodes are often used to improve diffusion into the dielectric (hygroscopic material). Basically, the hygroscopic material can be divided into three groups: ceramic, polymers and silicon. The most widely used ceramic is Al_2O_3 which presents good stability at high temperature and humidities [6]. The films of water insoluble polymer have been broadly used as hygroscopic

material although they have problems with hysteresis and stability for high temperature and humidities [7]. Adhikari *et al*. presented a review about the use of polymer in sensors [8]. The application of silicon as a hygroscopic material enables the integration of the humidity sensor with signal processing (MOS technologies). In this case one can find Si in the following forms: porous silicon [9], porous silicon carbide [10] and porous polycrystalline silicon [11].

- Resistive Humidity Sensor – theses sensors are based on the variation of the impedance as a function of amount water vapour absorbed. Similar to the capacitive, it can be divided into three groups: ceramics, polymers and electrolytic. The ceramic films have the ability to support higher temperature environment. There are many ceramic materials applied in humidity sensor, such as: $ZnCr_2O_4$-K_2CrO_4 [12], glass-ceramic of $LiTi(PO_4)_3$ [13] and thick film of Zn_2SnO_4-$LiZnVO_4$ [14]. Some films based on polymers have the disadvantage of not allowing to be applied to high humidity. Polymer materials applied in humidity sensor were presented in a review by Adhikari *et al* [8]. Finally, the electrolytic sensor can be represented by Dunmore sensor – also called as LiCl dew point sensor. This sensor has the disadvantage of not allowing be applied to low humidity [1].

The advancement of the fabrication process of IC and MEMS technology has allowed the development of thermal sensor for various applications such as: temperature sensors, pressure sensors and accelerometers. In the last years, micromachined thermal sensors based on the heat transfer mechanisms of conduction, convection (free or forced flow) and radiation have been developed using MEMS technology [15]. Actually, flow sensors for liquids and gases, based on MEMS technology are already successful commercial products. On the other hand, micromachined thermal sensors have still been under-explored as humidity sensors. Nowadays, there are various types of humidity sensors – employing different hygroscopic materials for sensing element.

In this work an air-humidity sensing element based on heat transfer mechanisms (conduction and convection) is presented, where the sensing element is a single floating resistor of doped polysilicon, which basically operates in two phases: thermal actuation and thermal sensing. As thermal actuator, a biasing current is applied to the resistor leading to its self-heating by Joule Effect. As thermal sensor, the biasing current is reduced and the cool-down process (conduction and convection) is measured trhough Thermal Time Constant (τ).

2. PHYSICAL PRINCIPLE OF THERMAL SENSOR

Thermal sensors measure physical quantities by transducing their signals into thermal quantities and then, transducing the thermal quantities into electrical quantities. A thermal sensor operates in three steps (with the exception of the temperature sensors, which transduce from the thermal to the electrical signal only): first, a non-thermal signal is transduced into a heat flow; second, the heat flow is converted into a temperature difference; and third, the temperature difference is transduced into an electrical signal using a temperature sensor [15]. In our case, a single polysilicon suspended resistor (floating resistor) was used as both: thermal actuator and thermal sensor element. Fig. 1 shows an schematic view of the floating polysilicon resistor.

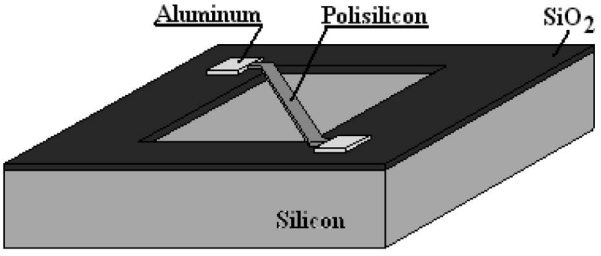

Figure 1. Three-dimensional view of the floating polysilicon resistor

During the thermal actuator phase, a convenient biasing current is applied to the floating resistor leading to its self-heating by Joule Effect. In the sensor configuration, the floating resistor biasing current is reduced and the time constant during the cool-down process is measured. This process will depend on the water vapor quantities in the ambient, since the resistor is suspended and cooling will be due to heat transfer mechanisms (thermal conduction and thermal convection). The heat transfer due to thermal radiation will not be considered in our analysis, since the sensor operates at low temperature.

3. HEAT TRANSFER MECHANISM

The heat transfer corresponds to the energy transferred due to a temperature gradient. The literature describes three different mechanisms for heat transfer: conduction, convection and radiation. Next, we describe the heat transfer due to conduction and convection (steady-state and transient).

3.1 Thermal Conduction Mechanism

Thermal conduction mechanism may be summarized as the transfer of energy from the more energetic to the less energetic particles of a substance due to interactions between the particles (diffusion). Higher temperatures are associated with higher molecules energies, and when neighboring molecules collide, as they are con-

stantly doing, an energy transfer from the more energetic to the less energetic molecules occurs. In the presence of a temperature gradient, energy transfer by conduction then occurs in the direction of decreasing temperature [17]. The equation that describes the heat transfer by conduction mechanism is give by:

$$q = -kA\frac{\partial T}{\partial x} \quad (1)$$

where, q is the heat flux [W], k the thermal conductivity [W/(m.K)] , A the transversal area of the floating resistor [m^2] and $\partial T/\partial x$ the temperature gradient [K/m].

In heat transfer analysis, transport and thermodynamic material properties should be taken into account. The transport properties include the diffusion rate coefficient such as the thermal conductivity (k). On the other hand, thermodynamic properties pertain to the system equilibrium state. Density (ρ) and specific heat capacity (C_p) are two properties used extensively in thermodynamic analysis. The thermal conductivity can be expressed by:

$$k = \alpha\rho C_p \quad (2)$$

where, α is the thermal diffusivity [m^2/s], ρ the density [Kg/m^3] and C_p the specific heat capacity [J/(Kg.K)].

Table I shows the thermal parameters of the materials [17] used in the sensor fabrication.

Table 1. Thermal Parameters [17].

Material Parameter	Si	SiO2	Si-poly	Al
Density (Kg/m^3)	2330	2220	2330	2702
Thermal Conductivity (W/m K)	148	1.38	125	237
Specific Heat Capacity (KJ/Kg K)	0.712	0.745	1.01654	0.903
Thermal Diffusivity (m^2/s)	89.2	0.834	0.165	97.1

The variation of the thermal conductivity of the air as a function of temperature and of the air-relative humidity, have been investigated since the 1950's [18]. Recently, P. T. Tsilingiris presented a study about the variation of the thermophysical properties of the air (density, viscosity, thermal conductivity, specific-heat capacity, thermal diffusivity and Prandtl number) as a function of the temperature and relative humidity of the air [19]. Table II presents some thermal properties of the air for 30, 40, 50 °C also considering 30, 50, and 80 %RH.

3.2 Thermal Convection Mechanism

Thermal convection mechanism is comprised of two mechanisms. In addition to energy transfer due to diffusion (conduction mechanisms), energy is also transferred by fluid motion – associated to a large number of molecules moving collectively. Such motion, in the presence of a temperature gradient, contributes to the heat transfer [19]. The equation that described the heat transfer by convection mechanism is give by:

$$q = hA_s(T_s - T_\infty) \quad (3)$$

where, q is the convective heat flux [W], h the convection heat transfer coefficient [W/(m.K)], A_s the surface area exposes with fluid (air in our case) and (T_s - T_∞) the difference between surface and fluid temperature, respectively.

Convection heat transfer may be classified according to the nature of the flow. Convection is said to be forced when the flow is caused by external means, such as by a fan, a pump or atmospheric winds. In contrast, for free (or natural) convection the flow is induced by buoyancy forces, which are due to density differences caused by temperature variations in the fluid.

3.3 Transient Analysis of the Heat Transfer

Consider that a solid is initially at a uniform temperature T_i and it is quenched by it in environment of lower temperature $T_\infty < T_i$. At the instant t = 0 start the cooling process and the temperature of the solid will decrease for time t > 0, until it reaches T_∞. This reduction is due to convection heat transfer at the solid-environment interface. In this case, we assume that the temperature of the solid is uniform at any instant during the transient process – this assumption implies that temperature gradient within the solid is negligible [21], in other words, this condition is closely approximate if the resistance to conduction within the solid is small compared with to the heat transfer resistance between the solid and its surroundings.

The temperature transient response is determined by formulating an overall solid energy balance. This balance must relate the rate of heat loss at the surface to the rate of the internal energy, which is given by:

$$-E_{out} = E_{in} \quad (4)$$

Table 2. Thermal parameters of the air [19].

Temp. (°C)		**30**			**40**			**50**	
Humidity (%RH)	**30**	**50**	**80**	**30**	**50**	**80**	**30**	**50**	**80**
Density (Kg/m^3)	1.16351	1.15713	1.15089	1.12682	1.11895	1.10789	1.08325	1.07568	1.05998
Thermal Conductivity (W/m.K)	0.02625	0.02621	0.02607	0.02689	0.02675	0.02666	0.02748	0.02738	0.02701
Specific Heat Capacity (KJ/Kg.K)	1.01245	1.01749	1.02289	1.01995	1.02770	1.03310	1.02129	1.03983	1.07890
Thermal Diffusivity ×10 $^{-6}$(m^2/s)	22.5	22.4	22.5	23.5	23.3	23.4	25.5	25.1	24.7

or

$$-hA_s(T-T_\infty)=\rho C_p V\frac{\partial T}{\partial t} \quad (5)$$

where, ρ is the density [Kg/m^3], C_p the specific heat capacity [J/(Kg.K)], V the volume of the floating resistor [m^3] and $\partial T/\partial x$ the temperature gradient [K/m].

Separation of variables and integrating from the initial condition (for $t = 0$ à $T(0) = T_i$), we then obtain:

$$\frac{T-T_\infty}{T_i-T_\infty}=e^{-\left(\frac{hA_S}{\rho C_p V}\right)t} \quad (6)$$

The foregoing results indicate that the difference between solid and environment temperature must decay exponentially to zero as t approaches to infinity. Note that the exponential decay will depend on the thermal parameters only if the difference in temperature between the solid and the environment remains constant and in this case, it is not necessary to use a different reference sensor to compensate for temperature variation in the environment.

In Eq. 6 the quantity ($\rho C_p V/hA_S$) may be interpreted as a Thermal Time Constant (τ) which can be expressed as:

$$\tau=\left(\frac{1}{hA_S}\right)\left(\rho C_p V\right)=R_t C_t \quad (7)$$

where, R_t is the resistance to convection heat transfer and C_t is the lumped thermal capacitance of the solid.

This behavior is analogous to voltage decay that occurs when a capacitor is discharged through a resistor in an *RC* circuit. Fig. 2 shows the electro-thermal model schematically represented by the *RC* circuit.

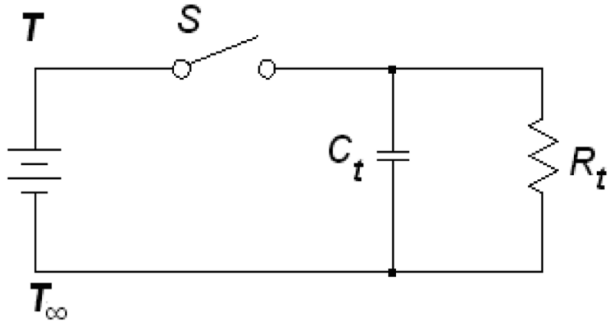

Figure 2. Electro-thermal model.

where, T is the temperature of the floating resistor and T_∞ the ambient temperature.

In our case, the heat transfer takes place by two ways: due to physical contact of floating resistor with its mechanical support and, due to the exposure of the floating resistor with the ambient (air). The thermal conduction, due to physical contact, is minimized because the floating resistor is fixed only at its extremities. On the other hand, the convection mechanism dominates the cooling process, because of the large area of the floating resistor, exposes to the ambient. Therefore, the convective heat transfer coefficient value depends on the resistor geometry, the fluid thermophysical properties, the fluid velocity and also on the temperature difference between the resistor and the environment [22]. Note that if the temperature difference remains constant in the transition from thermal actuator phase to thermal sensor phase, the values of the Thermal Time Constant (τ) will not change – depending only on the other parameters, according equation 7.

4. SENSOR FABRICATION

Basically, the fabrication of the floating resistor sensor is composed by four steps. The first step is the deposition of the SiO_2 sacrificial layer on a silicon wafer. This deposition is accomplished using a ECR-CVD system.

In the second step, a 1 μm thick polysilicon layer was deposited by vertical LPCVD at 800 °C using SiH_4 gas (40 sccm) diluted in H_2 (4800 sccm) and implanted with 3×10^{13} cm^{-2} boron dose at 40 keV ion energy. Rapid Thermal Annealing – RTA (1000 °C / 40 s) was used to activate the dopants and to restructure the crystalline lattice. The schematic cross-section view of the process after the polysilicon deposition is shown in Fig. 3.

Figure 3. Schematic of the floating polysilicon resistor fabrication – Polysilicon on SiO2 layer

In the third step, the resistor structure was defined by lithography and Reactive-Ion Etching – RIE (gas mixture of $SF_6/CF_4/N_2$, with flow ratio of 10:15:20, respectively). The etching time was 4 minutes and photolithographic process was carried out with the AZ3312 photoresist. After plasma-etching, another implantation, with a high boron dose (5×10^{15} cm^{-2}) was carried out. A second RTA step was used to active dopants.

Next, aluminum is evaporated and the contacts are defined by lift-off process, resulting in the structure shown in Fig 4.

Figure 4. Schematic of the floating polysilicon resistor fabrication – Definition of the region aluminum pads.

The last step is etching away the oxide layer under the polysilicon using buffered HF solution to get the suspended bridge. Fig. 5 shows the Micromachined Floating Resistor after all fabrication steps.

Figure 5. Schematic of the floating polysilicon resistor fabrication. Etching of sacrificial SiO_2 - Floating polysilicon resistor formed.

Fig. 6 shows a microscope image of the floating resistor. The sensor consists of a bridge-shaped doped polysilicon. The dimensions of the floating resistor are: 450 μm long, 75 μm wide and 1 μm thick.

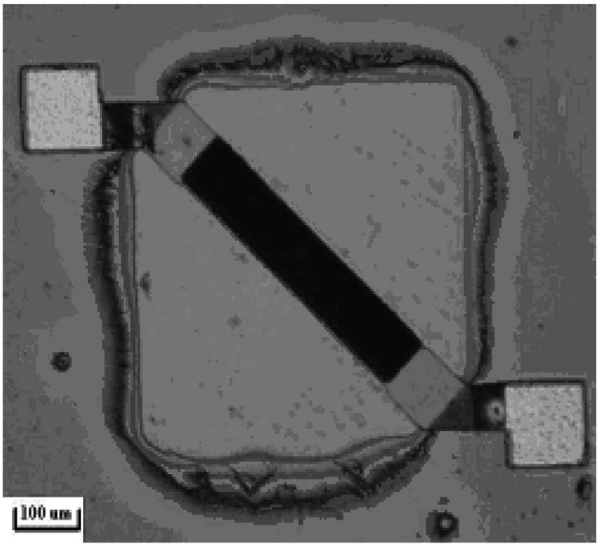

Figure 6. Microscope image of the floating resistor sensor

5. EXPERIMENTAL RESULTS

5.1 Temperaure Characterization of the Floating Resistor

The temperature characterization of the floating resistor was carried out in a climactic chamber (THERMOTRON – 3800), with temperature values between 15 °C and 55 °C, with steps of 5 °C. A multimeter (AGILENT – 34401A) was used to measure the resistance values of the floating resistor. Fig. 7 shows the resistance versus temperature curve.

The result can be fitted by the following equation:

$$R_{sen}(T) = 78637.77 - 341.76T + 0.93T^2 \quad (8)$$

where, $R_{sen}(T)$ is the resistance of the floating resistor and T the temperature.

Fig. 8 shows the TCR of the floating resistor versus temperature. The polysilicon TCR is dependent of the grain size of the polysilicon and of the boron doping concentration [22]. In our case, the floating resistor presents values from -0.425 to -0.380 %/°C in the temperature range between 15°C and 55°C.

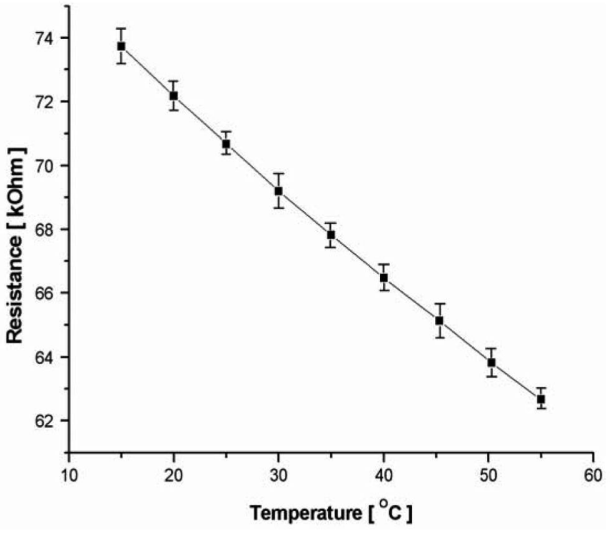

Figure 7. Resistance as a function of the Temperature

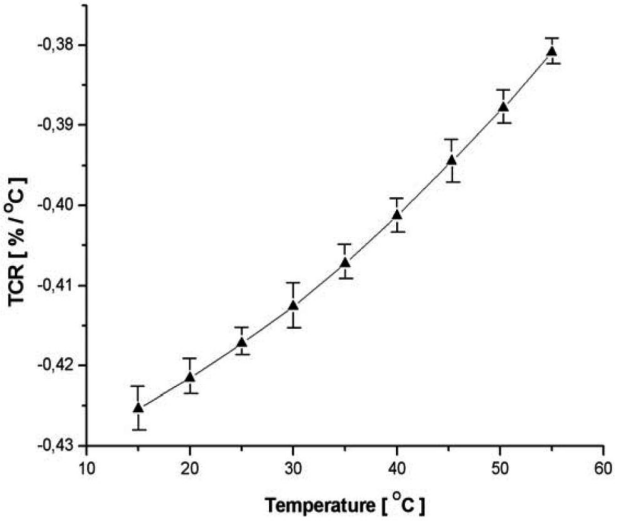

Figure 8. Floating resistor TCR versus temperature

5.2 Thermal Actuator Phase

In order to configure the floating resistor as a thermal actuator, we applied a convenient biasing current, leading to self-heating by Joule Effect. A voltage-to-current converter was used to characterize the thermal actuator. Fig. 9 shows the esquematic circuit.

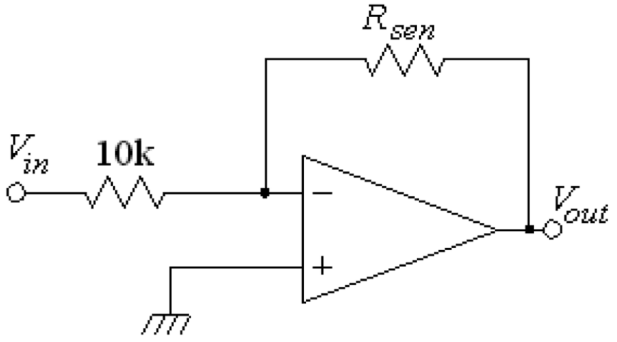

Figure 9. Schematic circuit for characterization of the thermal actuator

The 10k resistor used has a low value of TCR to ensure that only R_{sen} change. The resistance of the floating resistor (R_{sen}) is obtained by measuring the output voltage (V_{out}) as a function of the input voltage (V_{in}) and it is given by the following equation:

$$R_{sen} = -\frac{V_{out}}{V_{in}}10\text{k} \tag{9}$$

Fig. 10 shows the resistance of the floating resistor as a function of the input voltage. The floating resistor temperature is also show on the same figure (right axis). The equivalence between resistance and temperature is calculated based on Eq. 8. The test was performed until the floating resistor temperature heats up to approximately 50 °C. In this case, the input voltage was 2.8 V and maximum power consumption was 5 mW.

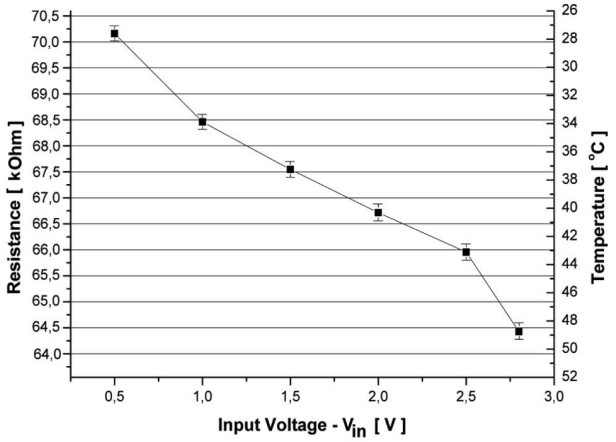

Figure 10. Resistance of the floating resistor versus input voltage

5.3 Thermal Sensor Phase

After thermal actuator phase, the input voltage is fixed at 0.5V and the cooling process is monitored during 30 seconds. The relative humidity and temperature were controlled using a climatic chamber (THERMOTRON – 3800).

The characterization of the floating resistor, R_{sen}, operating as a humidity sensor, was performed by measuring τ during the cooling process for different humidities (30 – 80%Rh) at room temperature and with atmospheric pressure of 703.6mmHg. Based on the capacitor charge/discharge theory (electro-thermal model), we define τ as the time required for the floating resistor to reduce the temperature in 37% (from 50 °C to 35.5 °C, in our case). Fig. 11 shows the dependence of the floating-resistor temperature, in the cooling process, for different humidities. We observe that, the cooling process presented an exponential response – in agreement the Equation 6. Table III resumes the Thermal Time Constant (τ) values for each %RH – represented graphically in Fig. 12.

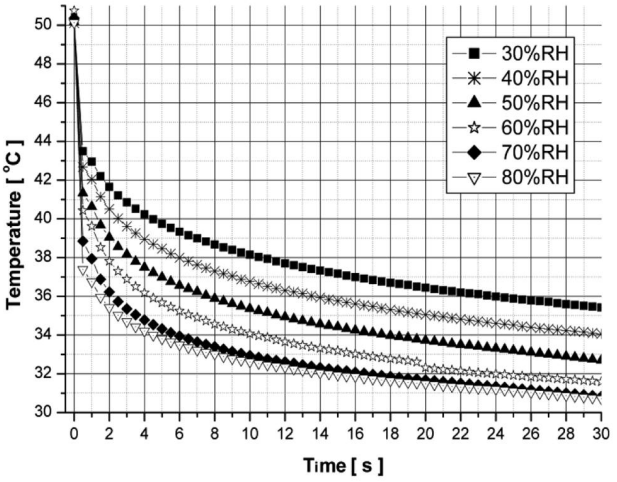

Figure 11. Cooling process of the floating resistor

Table 3: Thermal Time Constant values as a function of humidity.

%Rh	30	40	50	60	70	80
τ (s)	29	16.5	9.5	5.5	3	2

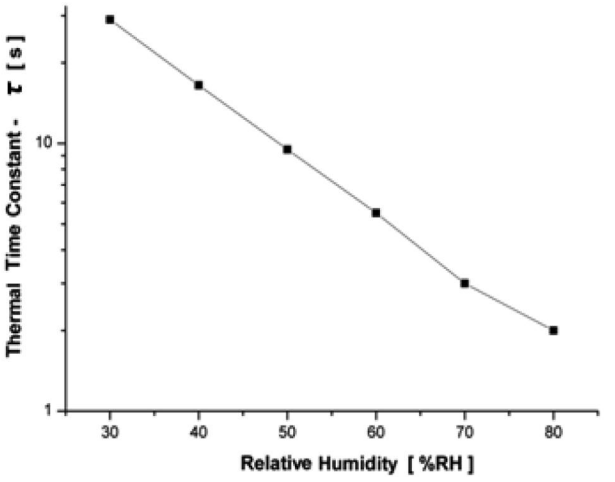

Figure 12. Thermal Time Constant (τ) versus Relative Humidity

6. CONCLUSION

We present a humidity sensor based on thermal transfer mechanisms (conduction and convection). Experimental results show that the cooling process, on the floating resistor, is dependent on the amount of water molecules (the convective heat transfer) in the environment since the temperature difference between the resistor and the environment remained constant, at the time of transition from thermal actuator phase to thermal sensor phase. Experimental results show that Thermal Time Constant (τ) is closely related to the relative humidity of the air surround the floating resistor. The floating resistor power consumption during the thermal actuator phase amounts to 5 mW.

ACKNOWLEDGEMENT

Authors acknowledge the Center for Semiconductor Components (CCS – UNICAMP) staff for the help in preparation of the samples. This work was financial supported by São Paulo State Research Foundation - **FAPESP** and the Brazilian National Research Council – **CNPq**, under National Institute of the Science and Technology for Intelligent Nano- and Micro-electromechanical system – **INCT-NAMITEC,** the Microlectronic National Program – **PNM (CNPq)**, and **Universal (CNPq)** Project n° 480864/2011-0.

REFERENCES

[1] Marvin, C. F. Moisture Tables. *American Meteorological Society*, Vol. 26, pp. 205-207, 1989.

[2] Rittersma, Z. M.. Recent achievements in miniaturized humidity sensor – a review of transduction techniques. *Sensors and Actuators A*. Vol.96, pp. 196-210, 2002.

[3] Schirmer, B. *et al*. High precision trace humidity measurements with a fibre-coupled diode laser absorption spectrometer at atmospheric pressure. *Meas. Science Technol.*, Vol. 11, pp. 382-391, 2000.

[4] Barstow, M. A., et al. The WSO, a word-class observatory for the ultraviolet. *Proc. SPIE –International Soc. Opt. Eng.*, Vol. 4854, pp. 364-374, 2002.

[5] Vetelino, K. A., *et al*. Improved dew point measurement based on a SAW sensor. *Sensors and Actuators B*, Vol. 35, pp. 24-31, 1996.

[6] Nahar, R. K. Study of the performance degradation of thin film aluminium oxide sensor at high temperature. *Sensors and Actuators B*, Vol. 63, pp. 49-54, 2000.

[7] Sakai, Y. Humidity Sensors based on polymer thin films. *Sensors and Actuators B*, Vol. 35, pp. 85-90, 1996.

[8] Adhikari, B. and Majumdar S. Polymers in sensors applications. *Prog. Polym. Sci.*, Vol. 29, pp. 699-766, 2004.

[9] O'Halloran, G. M.. Capacitive humidity sensors based on porous silicon. *Ph. D. Thesis*, TU Delft, 1999.

[10] Connolly, E. J. *et al*. Relative humidity sensor using porous SiC membranes and Al electrodes. *Sensors and Actuators B*, Vol. 100, pp. 216-220, 2004.

[11] Connolly, E. J. *et al*. Comparison of porous silicon, porous polysilicon and porous silicon carbide as materials for humidity sensor application. *Sensors and Actuators A*, Vol. 99, pp. 25-30, 2002.

[12] Bayhan, M. and Kavasoglu, N. A study on the humidity sensing properties of $ZnCr_2O_4$-K_2CrO_4 ionic conductive ceramic sensor. *Sensors and Actuators B*, Vol. 117, pp. 261-265, 2006.

[13] Nocun, M. and Bugajski, W.. Humidity sensor based on porous glass-ceramic. *Optical Applied*, Vol. 30, pp. 613-618, 2000.

[14] Fu, G. *et al*. Humidity sensitive characteristics of Zn_2SnO_4-$LiZnVO_4$ thick film prepared by the sol-gel method, *Sensors and Actuators B*, Vol. 81, pp. 308-312, 2002.

[15] Sani, E. A and Javan, D.. Analytical study of resistive MEMS gas flow meters. *Microsystems Technology.* Vol.14, pp. 89-94, 2007.

[16] Sze, S. M.. *Semiconductor Sensors*. John Willey & Sons, 1994.

[17] Incropera, F. P., *et al*. *Fundamentals of Heat and Mass Transfer*. 6th Edition. John Willey & Songs, 2008.

[18] Brokaw, R. S. Estimating thermal conductivities for nonpolar gas mixture. *Industrial and Eng. Chem.*, Vol. 47, pp. 2398-2400, 1955.

[19] Tsilingiris, P. T.. Thermophysical and transport properties of humidity air at temperature range 0 and 100 °C. *Energy Conversion and Management.* Vol. 49, pp. 1098-1110, 2008.

[20] Kimura, M. Absolute-humidity sensing independent of the ambient temperature, *Sensors and Actuators A*, Vol. 55, pp. 7-11, 1996.

[21] http://en.wikipedia.org/wiki/Biot_number

[22] Kreith, F., *et al*.. *Principle of Heat Transfer*. 6th Edition. Thomson Learning Ltda, 2003.

[23] French, P. J. Polysilicon: a versatile material for Microsystems. *Sensors and Actuators A*, Vol. 99, pp. 3-12, 2002.